Journal of Naval Architecture and Marine Engineering
Dec., 2020
http://dx.doi.org/10.3329/jname.v17i2.42622 *http://www.banglajol.info*

CFD ANALYSIS OF UNSTEADY PROPELLER PERFORMANCE OPERATING AT DIFFERENT INCLINED SHAFT ANGLES FOR LONG-TAIL BOAT IN THAILAND

P. Kaewkhiaw
Department of Maritime Engineering, Faculty of International Maritime Studies, Kasetsart University, Sri Racha Campus, 199 Moo 6, Sukhumvit Road, Tung Sukla, Sri Racha, Chonburi 20230, Thailand, Email: prachakon.ka@ku.th

Abstract:

Inclined shaft propeller arrangements are demonstrated in the high-speed boat. The flow field around the propeller blades with inclined shaft propeller is unsteady due to the cross-flow component from the influx of the shaft direction which complicated more than the straight shaft propeller condition (without inclined shaft angle). Therefore, realistic flow around inclined shaft propeller is important to predict the actual efficiency of propeller. In addition, propeller characteristics such as the pitch, skew and rake influence propeller performance. This paper offers the investigation of unsteady propeller performance operating at different inclined shaft angle conditions for Long-Tail Boat (LTB) using a Reynolds Averaged Navier-Stokes (RANS) solver. The unsteady calculations are conducted considering inclined flow conditions. The computational results of propeller performance and pressure distribution on the suction and pressure sides at the blades with time-accuracy have been compared to each other including the wake effect behind the propeller. The results can be applied to adjust the inclined shaft angle of the boat.

Keywords: LTB, RANS, CFD, inclined shaft propeller, unsteady propeller performance.

NOMENCLATURE

LTB	Long-Tail Boat
CFD	Computational fluid dynamics
RANS	Reynolds-Averaged Navier–Stokes
EVMs	Eddy-Viscosity models
RSMs	Reynolds-Stress models
SST *k-ω*	Shear Stress Transport *k-ω*
T	Thrust of propeller
Q	Torque of propeller
K_T	Propeller thrust coefficient
K_Q	Propeller torque coefficient
J	Advance coefficient
n	Propeller rotational speed
V_A	Uniform inflow velocity
η_o	Propeller efficiency

Greek symbols

$-\rho\overline{u_i'u_j'}$	Unknown Reynolds Stresses
μ_t	Eddy Viscosity
k	Kinetic energy
δ_{ij}	Kronecker delta
G_ω	Generation of ω
Γ_k	Effective diffusivity of k
Γ_w	Effective diffusivity of ω
Y_k	Dissipation of k due to turbulence
Y_ω	Dissipation of ω due to turbulence
D_ω	Cross-diffusion term
S_k, S_ω	User-defined source terms
$\overline{G_k}$	Generation of turbulence kinetic energy due to mean velocity
ω	Specific dissipation rate
ρ	Density of fluid

1. Introduction

Long-Tail Boat (LTB) is the regional boat in Thailand which is high speed vessel. Actually, the operating speed is equal to approximately 27 knots. It carries passenger and tourist in the river. Fig. 1 shows the Long-Tail Boat studied in this research. It has been plying on the Chao Phraya River in Bangkok, Thailand. It has length, breadth, depth, and draft of 8.88 m, 1.60 m, 0.72 m and 0.27 m respectively. The engine is set to the stern of the boat with an inboard engine which connects the long shaft propeller. The shaft length is 4.5 m. The propeller is

1813-8235 (Print), 2070-8998 (Online) Received on: Aug., 20219

attached to the end of a long shaft with two blades. Because of shallow water, the boat is operated with an inclined shaft propeller. The actual inclined shaft angle is about 12°.

Fig. 1: Typical photograph of Long-Tail Boat

The brief summary of the experiments for operating at inclined shaft angle conditions have been long time interested such as the experimental evaluation of the propeller cavitation with many propeller models operating at inclined shaft angle of 4° and 8° (Taniguchi et al., 1967). Alder and Moore (1977) conducted propeller performance (P4407) operating at inclined shaft angle 19.5° at different shaft yaw angles -9.75°, 5°, 9.75° and 19.5°. Boswell et al. (1981, 1984) presented the measurement of performance for the single blade load on a moderate skewed propeller (DTMB 4661) operating in oblique flows of 10°, 20° and 30° for which experimental data are used to the validation for the potential propeller analysis codes by many researchers. Next, the measurement of the pressure distribution on two propeller models (DTMB 4679 and DTMB 4718) operating at inclined shaft angle of 7.5° from the horizontal axis is proposed by Jessup (1982). In addition, DTMB 4679 results are summarized in 22nd ITTC propulsion committee propeller RANS/Panel method workshop. After that, Raestad (2007) analyzed blade forces for DNV including the one blade thrust, torque, transverse force, bending moment and spindle moment on 4 blades for low skewed propeller operating in oblique flow of 10° and behind wake screens providing V-shape axial wakes.

Concurrently, the numerical methods were applied to investigate the propeller performance including cavitation for operating at inclined shaft angle conditions. Kinnas and Pyo (1998) proposed the first harmonic of forces and moments acting on a blade including the cavity shape for DTMB 4661 for operating at inclined shaft angles 10° and 20° based on vortex lattice method. Dubbioso et al. (2013) offered the analysis of propeller performance for E779A INSEAN model in oblique flow using CFD code χnavis. Kaewkhiaw and Ando (2014) presented the numerical calculation of propeller performance for thrust and torque coefficients with the P4990 in unsteady flows for operating at inclined shaft angles 4.8° and 8.8° based on RANS solver. After that, they calculated the unsteady propeller pressure distributions in terms of mean pressure distribution, first harmonic amplitude and first harmonic phase angle for DTMB 4679 operating at inclined shaft angle of 7.5°. Kaewkhiaw et al. (2016) evaluated Thai Long-Tail Boat propeller performance for operating at inclined shaft angle of 12°. Furthermore, the effect of shaft yaw angles on propeller performance at inclined shaft angle of 12° for Thai Long-Tail Boat are studied using CFD by Kaewkhiaw (2018).

The actual Long-Tail Boat Propeller (LTBP) is determined to have an inclined shaft angle approximately 12° by local wisdom which has never been studied before. Therefore this paper presented the RANS numerical method to investigate the unsteady propeller performance of LTB operating at straight shaft condition and compared with those for different inclined shaft angle conditions. In addition to the propeller performance, pressure distribution on suction and pressure sides of the blades at each different inclined shaft angle conditions are compared to each other including the wake.

2. Long-Tail Boat Propeller (LTBP) Model

The principal particulars of the Long-Tail Boat propeller model are shown in Table 1. Fig. 2 presents the propeller model of Long-Tail Boat. The model test is conducted by using the high speed circulating water channel at Kyushu University for operating at straight shaft angle by Kaewkhiaw et al. (2016). Propeller rotational speed is fixed at 10 rps. The measurements are taken for the ranges of the advance coefficients, J are from 0.5 to 1.4. Unfortunately, the experiments were not measured at inclined shaft conditions because the limit of equipment.

Table 1: Principal particulars of Long-Tail Boat propeller

Model name	Long-Tail Boat Propeller
Type of propeller	Fixed Pitch
Numbers of blade	2
Diameter [mm]	200
Expanded area ratio	0.6
Pitch ratio at 0.7R	1.289
Direction of rotation	Right Hand
Design advance coefficient [J]	1.1

Propeller geometry parameters

r/R	P/D	Rake/D	θ_S	c/D
0.14	0.873	-0.013	0.000	0.458
0.20	0.909	0.010	0.000	0.501
0.30	1.018	0.021	6.768	0.541
0.40	1.101	0.027	11.570	0.600
0.50	1.192	0.035	15.679	0.621
0.60	1.221	0.042	19.593	0.613
0.70	1.260	0.048	22.585	0.583
0.80	1.268	0.051	24.925	0.519
0.90	1.274	0.055	27.328	0.392
1.00	1.206	0.062	29.571	0.044

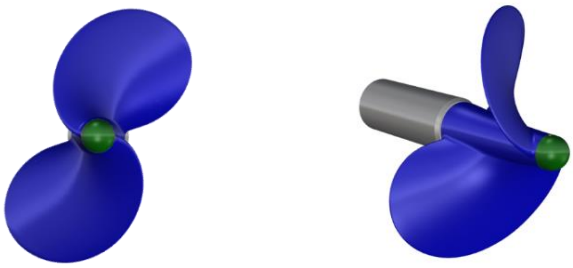

Fig. 2: Long-Tail Boat propeller model at front view (left) and isometric view (right)

The flows and force components with inclined shaft propeller corresponding to this work is shown in Fig. 3. The inflow velocity, V_{in} is divided into two components on the propeller shaft plane, the first is $V_{in} \cos\psi$ in the shaft axial direction. The second is $V_{in} \sin\psi$ in vertical direction of the propeller shaft. Here ψ is the inclined shaft angle to the horizontal axis. The propeller generates the axial thrust, T which can be divided into two components. T $\cos\psi$ is the thrust component to push the vessel forward along the horizontal axis and T $\sin\psi$ is along the vertical axis.

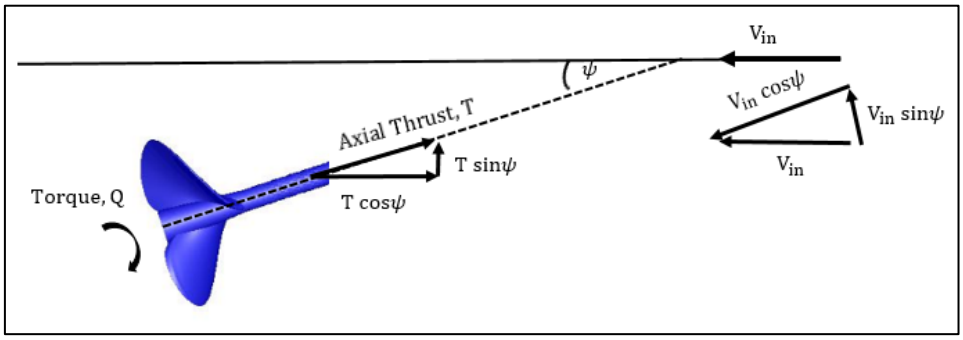

Fig. 3: Flow velocity and force propeller diagram for LTBP

3. Numerical Methods

The incompressible flow is solved with the conservation of mass and momentum. The conservation equations have ordinarily known as Navier-Stokes Equations (RANS). The continuity equation of RANS can be written as follows:

$$\frac{\partial \rho}{\partial t} + \frac{\partial (\rho u_i)}{\partial x_i} = 0 \tag{1}$$

The momentum equations form as follows:

$$\frac{\partial (\rho u_i)}{\partial t} + \frac{\partial (\rho u_i u_j)}{\partial x_j} = -\frac{\partial p}{\partial x_i} + \frac{\partial}{\partial x_j}\left[\mu\left(\frac{\partial u_i}{\partial x_j} + \frac{\partial u_j}{\partial x_i} - \frac{2}{3}\delta_{ij}\frac{\partial u_i}{\partial x_i}\right)\right] + \frac{\partial}{\partial x_j}\left(-\rho\overline{u_i' u_j'}\right) \tag{2}$$

The RANS models can be classified into two groups: Eddy-Viscosity Models (EVMs) and Reynolds-Stress models (RSMs). EVMs are based on the Boussinesq hypothesis where the Reynolds stresses are proportional to the rates of strain form as follows:

$$-\rho\overline{u_i' u_j'} = \mu_t\left(\frac{\partial u_i}{\partial x_j} + \frac{\partial u_j}{\partial x_i}\right) - \frac{2}{3}\rho k \delta_{ij} \tag{3}$$

Where μ_t is eddy viscosity, k is the kinetic energy of turbulence and $\delta_{ij}$is the Kronecker delta $\left(\delta_{ij} = 1\ if\ i = j\ and\ \delta_{ij} = 0\ if\ i \neq j\right)$. The Shear Stress Transport, SST *k-ω* turbulence model is applied to calculate Reynolds-Stress term in the RANS equations. The SST *k-ω* equations are written as follows:

$$\frac{\partial}{\partial t}(\rho k) + \frac{\partial}{\partial x_i}(\rho k u_i) = \frac{\partial}{\partial x_j}\left(\Gamma_k \frac{\partial k}{\partial x_j}\right) + G_k - Y_k + S_k \tag{4}$$

$$\frac{\partial}{\partial t}(\rho \omega) + \frac{\partial}{\partial x_j}(\rho \omega u_j) = \frac{\partial}{\partial x_j}\left(\Gamma_\omega \frac{\partial \omega}{\partial x_j}\right) + G_\omega - Y_\omega + D_\omega + S_\omega \tag{5}$$

Where G_k is the production term of turbulence kinetic energy due to mean velocity gradients, G_ω is that of ω, Γ_k and Γ_ω are the effective diffusivity of k and ω respectively. Y_k and Y_ω are the dissipation term of k and ω due to turbulence, D_ω is the cross diffusion term.

The SST *k-ω* is developed to efficiently fusion the study and accurate formulation in the near-wall regions with the free stream independence at the far-field therefore that potentiality to react the Low-Reynolds at near-wall regions and High-Reynolds at far-field regions. Furthermore, theirs can compute to more accurately for non-equilibrium areas in boundary layers with adverse pressure gradients such as separation domains. The computational fluid dynamics code ANSYS Fluent is employed in this research study. The governing equations are discretized by using the finite volume method. The pressure-velocity coupling is achieved through the

SIMPLE algorithm. The Second Order Upwind scheme is imposed for the discretization of the momentum equation. The discretized equations are solved by using Gauss-Seidel iterations.

4. Computational Domains and Grid Generation

The realistic flow around the propeller operating at inclined shaft arrangement is not symmetrical therefore the computational domain should be considered to whole domains with oblique flow. The computational domain with full blade propellers operating at inclined shaft conditions is presented in Fig. 4. It is split into two regions, i.e., the rotating and fixed parts. The rotating part is called "Rotating" and the fixed part "Stationary". The inflows velocity, V_{in} have been decomposed into velocity components which are defined as $V_x = V_{in}\cos\psi$ and $V_z = V_{in}\sin\psi$. The inclined shaft angle conditions, ψ are considered between 8° to 30° for this study because it has corresponded to the practical application of the Long-Tail Boat. Inlet position is determined to inflow velocity and outlet position imposed to constant static pressure equal to zero. The propeller shaft length in the calculation domain has been resized into the same ratio of propeller scale. The computational domain dimensions are presented in Table 2 which was studied by Kaewkhiaw et al. (2016).

The mesh motion systems have been analyzed to evaluate the unsteady propeller performance with time accuracy. The oblique inflow is conducted to each time step in the time domain. The propeller rotation angle varied one degree per time step size (0.0002777 seconds per a degree). Turbulence intensity and turbulence viscosity at inlet boundary are prescribed to 1%. No-slip boundary condition is set for solid surfaces (blade and hub) and the free-slip boundary condition is imposed for outer surface.

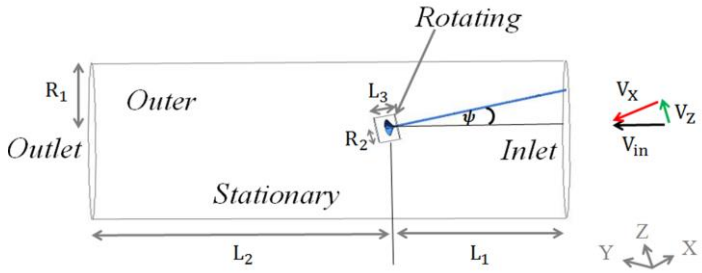

Fig. 4: Computational domains with operating inclined shaft propeller condition

Table 2: Computational domain dimensions with operating inclined shaft propeller condition

	Rotating	Stationary
L_1		10.43D
L_2		16.63D
L_3	1.17D	
R_1		4.41D
R_2	0.73D	

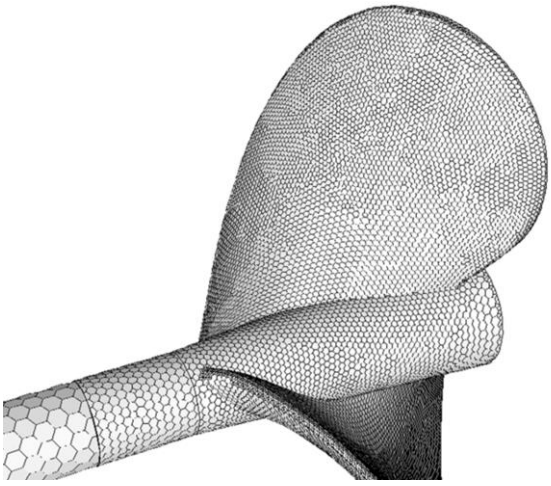

Fig. 5: Polyhedral cells on the propeller blade and hub

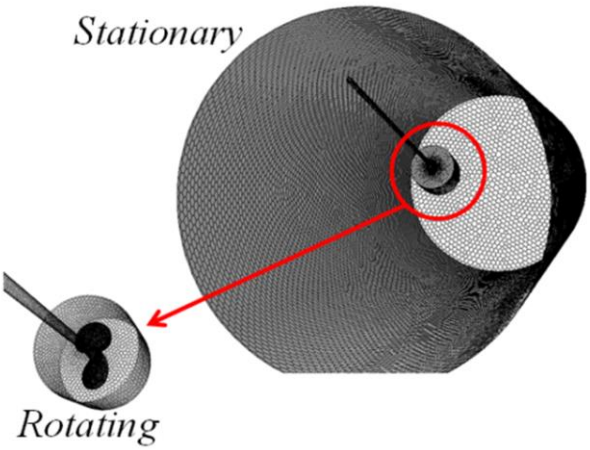

Fig. 6: Computational domains grid for rotating and stationary parts

The computational domains of rotating and stationary regions are generated by polyhedral volume cells. The blade and hub surfaces are defined to fineness grid with small polyhedral cells and the other surfaces imposed

grid bigger than blade and hub. The surface grid on a propeller blade is shown in Fig. 5. The grid quality of computational domains with Long-Tail Boat propeller has been analyzed by Kaewkhiaw (2018). Therefore, this research applied the grid of about 3M cells for total grids which are separated into the rotating and stationary regions by approximately 2M and 1M cells respectively. Fig. 6 shows the grid of calculation domains.

The numerical simulations are carried out on the personal computer with a 64-bit processor, Intel(R) Core(TM) i7-4790, CPU@3.60GHz, and 16 GB RAM. The processing time of calculation by the parallel processor (8 CPU) are employed about 48 hours per an advance coefficient for 6 cycles of propeller rotation with achieving residual convergence requirement of $1e^{-06}$ in all cases.

5. Test Problems Description with Unsteady Flow

The numerical results of unsteady propeller performance are conducted to operating with the straight shaft condition (without inclined shaft angle) and operating with the different inclined shaft angle conditions comparing to each other including the experiment. The unsteady flow calculations have been performed in uniform inflow operating at different inclined shaft angles. The angle of propeller rotation is set one degree per time step. The propeller thrust and torque have been transformed into the inflow direction because this is a push to the boat forward. Fig. 7 shows the experiment and calculation results of average thrust and torque coefficients operating at straight shaft condition including the inclined shaft angles between 8° to 30°. It seemed the thrust and torque coefficients operating at straight shaft condition between calculation results (black solid line) and measurement (black circle point) are agreed well at each range of advance coefficients including at design advance coefficient, (J=1.1). The advance coefficient is determined in the equation by using oblique flow velocity. Therefore, it is found that the advance coefficient has low value with the high inclined shaft angles.

The thrust coefficient lines with high inclined shaft angles, ψ = 20° to 30° are slightly lower than operating the straight shaft condition at J<0.8 but it showed higher than the straight shaft condition at J>0.8. Unfortunately, the testing of different inclined shaft angles was not measured because the limitation of apparatus in the experiment. It is found that, the thrust coefficient lines with low inclined shaft angles, $\psi \leq 15°$ were almost showed as same to the straight shaft condition (black solid line) including the experiment (black circle point) at J<0.9 but the thrust coefficient lines are slightly more than those with the straight shaft condition at J>0.9. It is clearly seen that the trend of inclined shaft angle is high the value then the thrust coefficient will grow up at the higher advance coefficient which flow has high speed.

Meanwhile, the torque coefficient lines with high inclined shaft angles, ψ = 25° and 30° are lower than those for operating at the straight shaft condition at J<0.8 which are also true for the thrust coefficient. However, the values showed higher than the straight shaft angle at J>0.8. The low inclined shaft angle conditions, $\psi \leq 15°$ have demonstrated the values increasing than the straight shaft condition at each range of advance coefficients. Then, it is found that the high value of inclined shaft angle, the torque coefficient is raised at the higher advance coefficient.

The propeller efficiency lines with the different inclined shaft angles are presented in Fig 8. It found that the numerical results (black solid line) and the experiment (black circle point) operating at straight shaft condition is a good agreement. The values with high inclined shaft angles, ψ = 20° to 30° showed over more than those for operating at the straight shaft angle condition at J>0.9 including at design advance coefficient. Furthermore, the efficiency of the high value of inclined shaft angle is showed increasing than those for operating at the low value of inclined shaft angle, especially at the higher advance coefficient. However, the propeller efficiency was not differed between for operating at the straight shaft and inclined shaft angles at the lower advance coefficients, J<0.9 which is low speed flow.

Actually, Long-Tail Boat propeller is set inclined shaft angle, ψ = 12° which found that the thrust and torque coefficients lines are slightly increased than the straight shaft angle at each range of advance coefficients. The one reason of that results above because the propeller characteristics such as the pitch, skew and rake cannot be operated in design condition (propeller characteristics have been designed by without inclined shaft angle)

therefore the propeller performance has been generated to inconstancy.

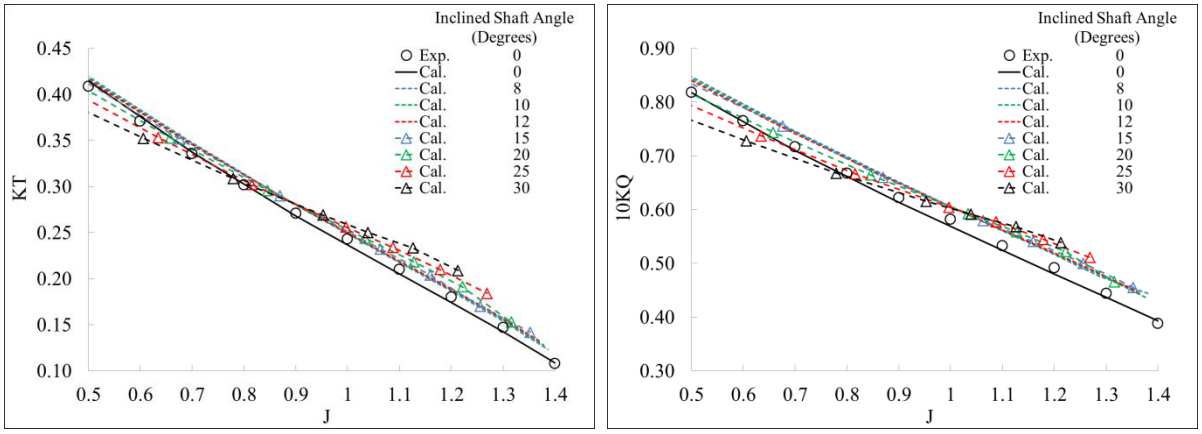

Fig. 7: Comparison of average thrust (left) and torque coefficients (right) for operating at different inclined shaft angle conditions

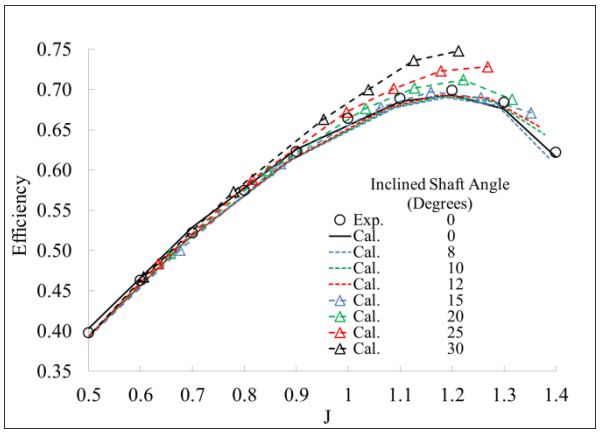

Fig. 8: Comparison of propeller efficiency for operating at different inclined shaft angle conditions

The computational results of actual thrust and torque coefficients as one rotational operating at different inclined shaft angles at design advance coefficient is shown in Fig. 9 which corresponded in Fig. 7. It seems the high inclined shaft angles showed the amplitude of thrust and torque coefficients more than those with the low inclined shaft angles. The maximum and minimum of two periods can found at blade position about 120º, 300º and 60º, 240º degrees respectively. Moreover, the fluctuated value of the high inclined shaft angles is generated more than those with the low inclined shaft angles.

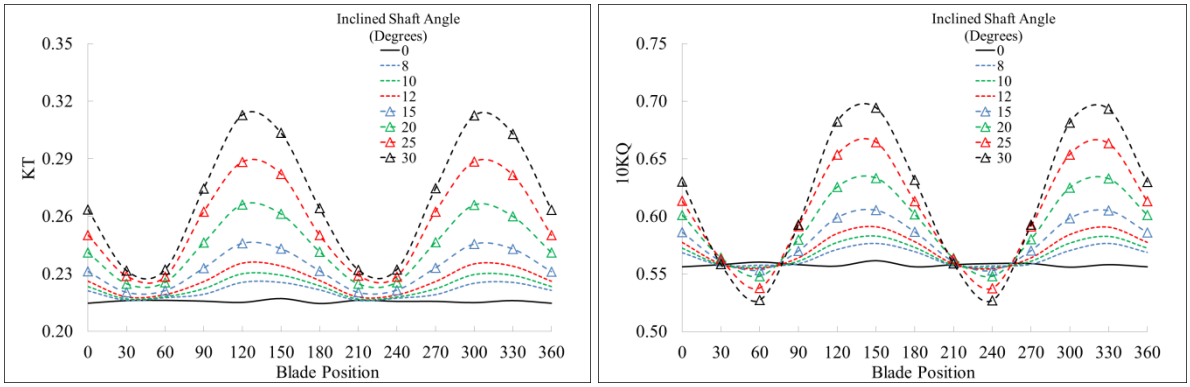

Fig. 9: Comparison of thrust (left) and torque coefficients (right) as functions of blade position at design advance coefficient and operating at different inclined shaft angle conditions

Figs 10 to 12 show the comparison of calculation results for pressure coefficient distributions on the blade, r/R = 0.5, 0.7 and 0.9 operating at different inclined shaft angles at the design advance coefficient for the angular

blade position about 0º, 120º and 240º respectively which corresponded to propeller performance in Fig. 6. It seemed the angular blade position about 0º, the pressure at pressure side in x/C = 0.2 to 0.7 on the r/R = 0.5 (middle of the blade) operating the high inclined shaft angles (marker line colors) including the actual inclined shaft angle, ψ = 12° were increased than the straight shaft angle. But, the pressure at suction side of it in x/C = 0.2 to 0.5 seemed slightly decreased from the straight shaft angle. On the r/R =0.7 and 0.9 (near the tip blade), the pressure at pressure and suction sides operating the high inclined shaft angles and low inclined shaft angles including the straight shaft angle were similar values.

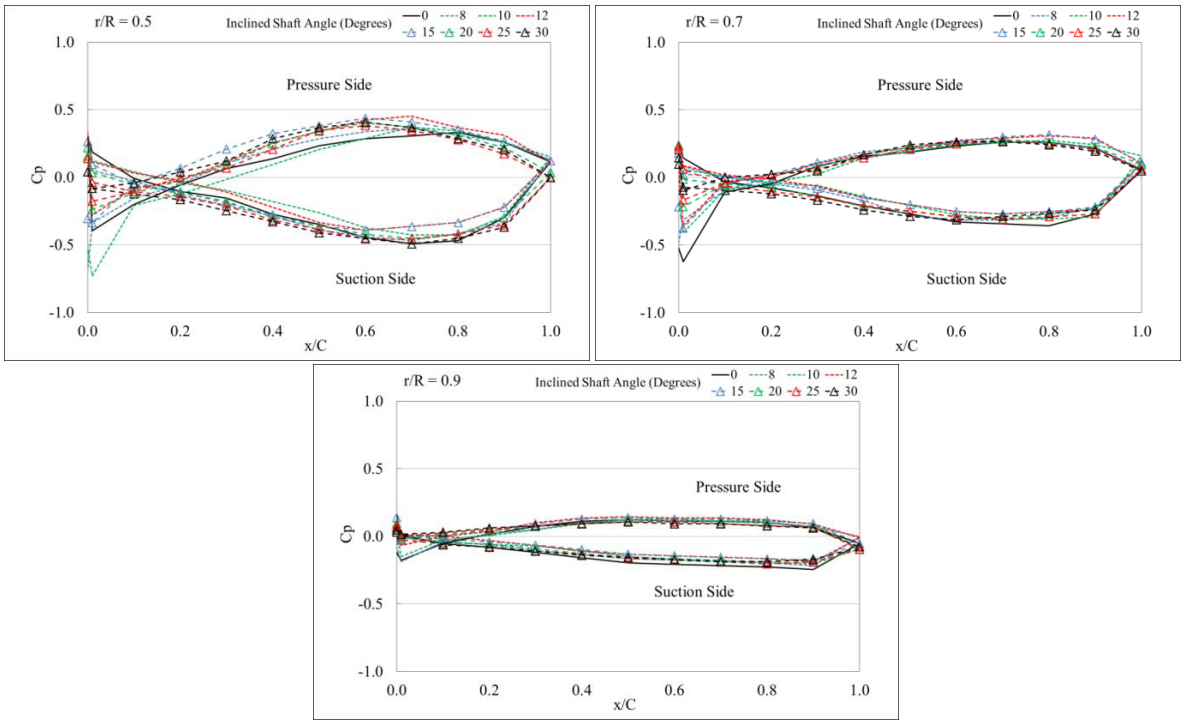

Fig. 10: Chordwise distribution of pressure coefficients on the blade, r/R=0.5, 0.7 and 0.9 at design advance coefficient for the angular blade position about 0º and operating at different inclined shaft angles

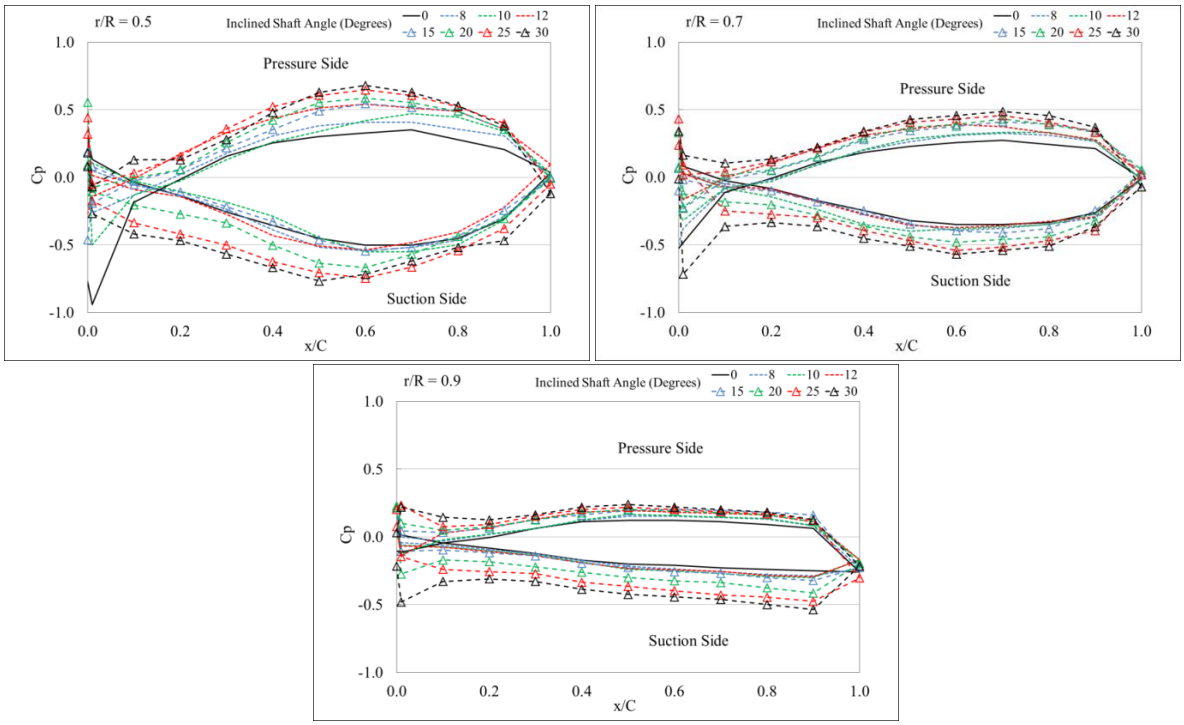

Fig. 11: Chordwise distribution of pressure coefficients on the blade, r/R=0.5, 0.7 and 0.9 at design advance

coefficient for the angular blade position about 120º and operating at different inclined shaft angles

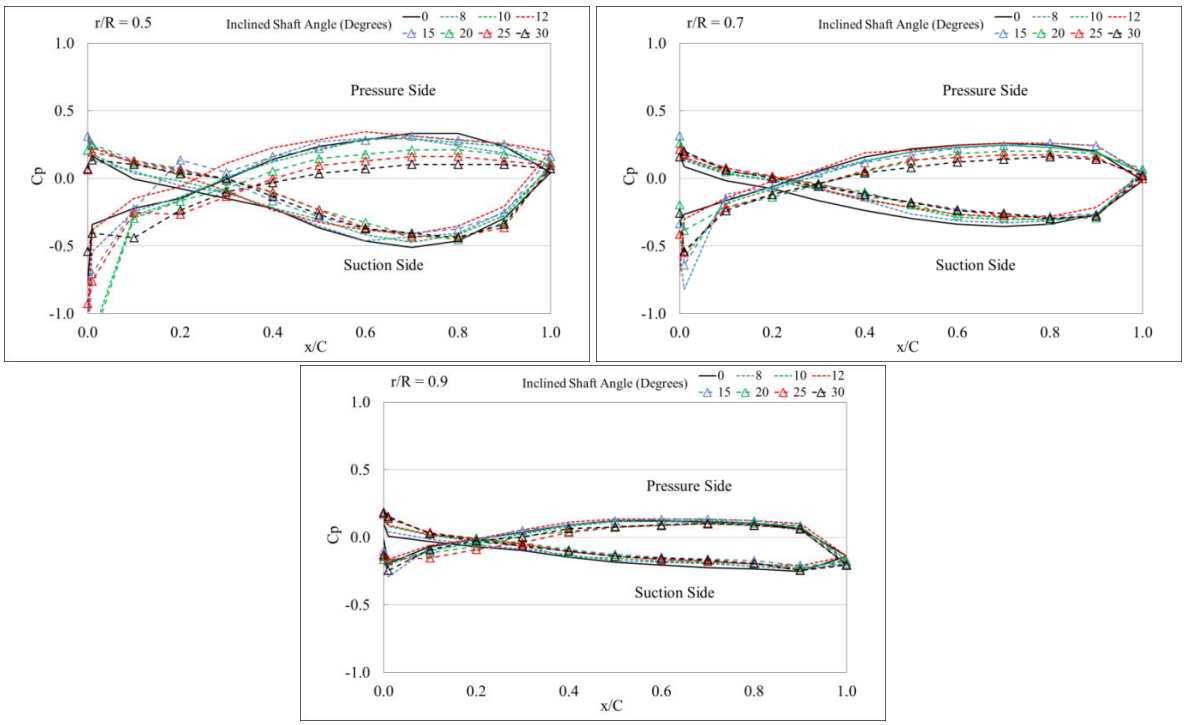

Fig. 12: Chordwise distribution of pressure coefficients on the blade, r/R=0.5, 0.7 and 0.9 at design advance coefficient for the angular blade position about 240º and operating at different inclined shaft angles

The angular blade position about 120º, it is clearly seen that the pressure at pressure side in x/C = 0.1 to 0.9 on the r/R = 0.5, 0.7 and 0.9 operating the all inclined shaft angles are increased than operating the straight shaft angle. Furthermore, the pressure of it with the high inclined shaft angles (marker line color) is higher than those with the low inclined shaft angles. The pressure at suction side in x/C = 0.1 to 0.9 on the r/R = 0.5, 0.7 and 0.9 operating the high inclined shaft angles were decreased from the straight shaft angle. It is seen that the pressure at suction side with the actual inclined shaft angle, ψ = 12° and the straight shaft angle were showed similarly.

The angular blade position about 240º, the pressure at pressure side in x/C = 0.4 to 0.9 on the r/R = 0.5 and 0.7 operating the high inclined shaft angles were showed decreasing than the straight shaft angle. The pressure at suction side in x/C = 0.4 to 0.8 are demonstrated increasing than the straight shaft angle. It found the actual inclined shaft angle, ψ = 12° showed similar to the straight shaft angle. On the tip blade at r/R = 0.9, the pressure at pressure and suction sides were displayed no difference between the straight shaft and inclined shaft angles.

Figs 13 to 15 present the comparison of computational results for pressure coefficient distributions at the propeller blades on suction and pressure sides at design advance coefficient operating at different inclined shaft angles as the angular blade position approximately 0º, 120º and 240º respectively. It is clearly seen that the shape of pressure distributions on each blade of propellers are similar for operating the straight shaft angle because no effect of unsteady forces with inclined shaft angles. However, the pressure distribution contours are found different on each blade of propellers when considered for the inclined shaft angle. Furthermore, the large difference pressure distributions of them are shown operating at high value of inclined shaft angles because of that each blade generated the unbalanced loading more than those for operating at low inclined shaft angles. In addition, this phenomenal is induced to the beginning of cavitation on the blade which led to damage of the propeller.

Fig. 16 shows the comparison of the pressure coefficients on the blades including the long shaft propeller at design advance coefficient for the inclined shaft angle, ψ = 12° (actual) and the inclined shaft angle, ψ = 30° (maximum). The shape of pressure distributions on each blade of propellers with inclined shaft angle, ψ = 30° indicates much more difference than those with inclined shaft angle, ψ = 12°, especially at pressure side.

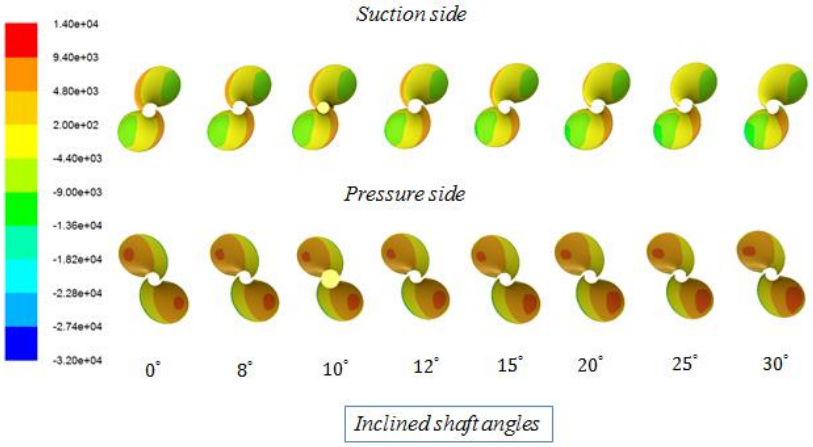

Fig. 13: Contours of pressure coefficient on suction and pressure sides at design advance coefficient for the angular blade position about 0º and operating at different inclined shaft angles

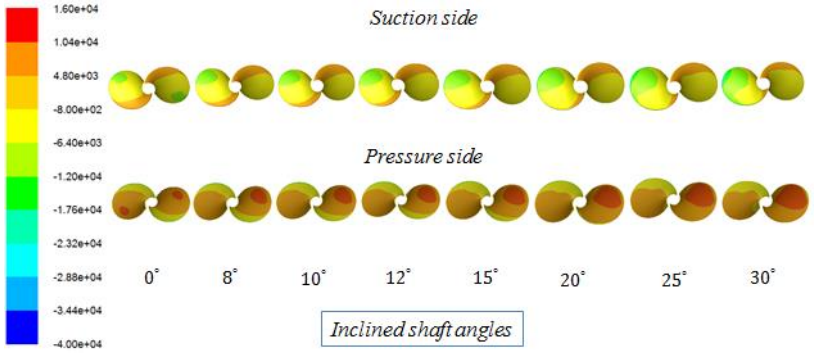

Fig. 14: Contours of pressure coefficient on suction and pressure sides at design advance coefficient for the angular blade position about 120º and operating at different inclined shaft angles

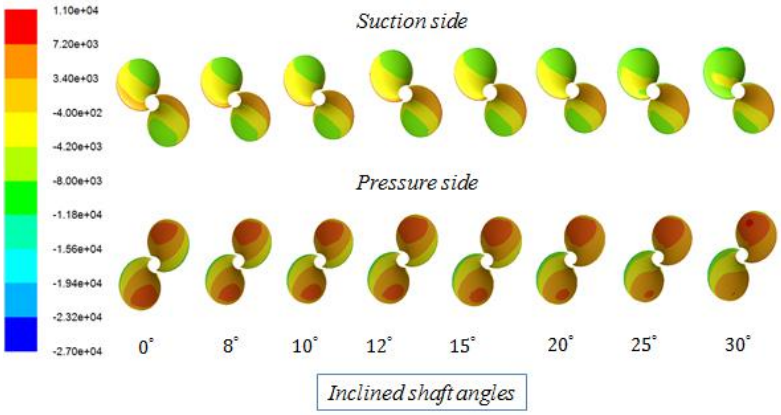

Fig. 15: Contours of pressure coefficient on suction and pressure sides at design advance coefficient for the angular blade position about 240º and operating at different inclined shaft angles

The propeller wake is analyzed through velocity magnitude contours. The axial velocity fields in the downstream of the blades with cutting plane cross the propeller at x/R =0.3 at design advance coefficient and operating at different inclined shaft angles for the angular blade position approximately 0º, 120º and 240º are provided in Fig. 17. It seemed the velocity contours in the propeller plane can be similar to each blade of propellers for the straight shaft angle. However, it showed high value including many differences behind the blade areas for the inclined shaft angle. Moreover, the higher inclined shaft angle showed different velocity distributions in the plane more than those for operating at lower inclined shaft angle consequently. It has been

developed to unbalance forces including the primary cause of cavitation as shown in Figs 13 to 15.

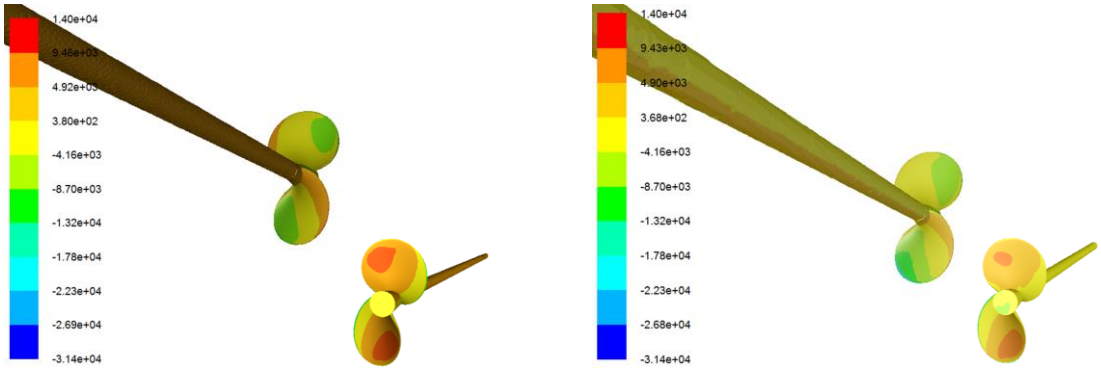

Fig. 16: Shapes of pressure coefficient for LTBP at the design advance coefficient for operating at inclined shaft angle, ψ = 12° (left) and the inclined shaft angle, ψ = 30° (right)

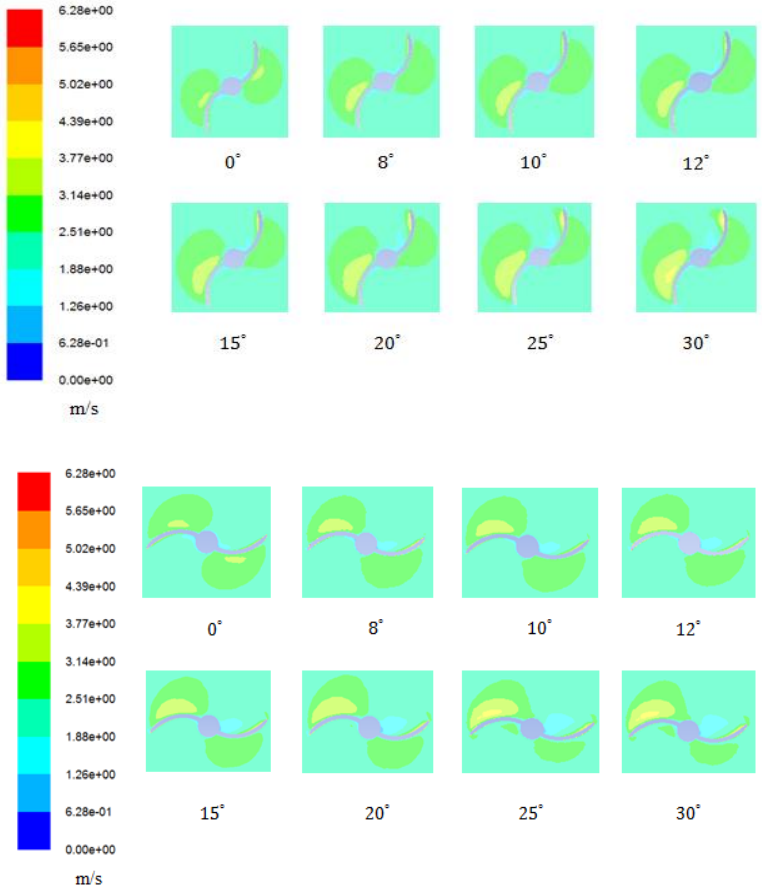

Fig. 17(a): Shapes of velocity magnitude in the downstream of the propeller, x/R = 0.3 at the design advance coefficient for the angular blade position about 0º (top) & 120º (bottom) and operating at different inclined shaft angles

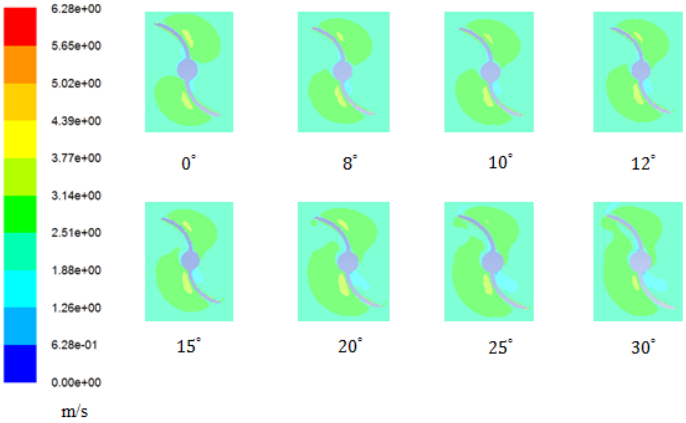

Fig. 17(b): Shapes of velocity magnitude in the downstream of the propeller, x/R = 0.3 at the design advance coefficient for the angular blade position about 240º and operating at different inclined shaft angles

6. Conclusions

The unsteady propeller performance of LTB operating at straight shaft angle and the different inclined shaft angle conditions are evaluated in detail. It is found that the numerical results of propeller performance with the straight shaft angle are in very good agreement with experimental results at each range of advance coefficients including design advance coefficient.

At high inclined shaft angles, $\psi \geq 20°$, the numerical results of the average thrust and torque coefficients are slightly lower than those with straight shaft ($\psi = 0°$) and experimental values at J<0.8 (low speed). But those are seemed to increase at J>0.8 (high speed). Meanwhile, the thrust coefficient operating at low inclined shaft angles, $\psi < 20°$ showed similarity to the straight shaft ($\psi = 0°$) at J<0.9 but it is slightly increased at J>0.9. The torque coefficient operating at low inclined shaft angles, $\psi < 20°$ are more than those with the straight shaft condition at each range of advance coefficients. It is found that the propeller efficiency operating at high inclined shaft angles are higher than those at the low inclined shaft angles including the straight shaft condition at J>0.9 (high speed). The reason behind it is that the propeller characteristics such as propeller pitch, rake and skew have been not designed to working in design propeller condition for inclined shaft angle. Therefore, the tendency of thrust and torque coefficients for the high inclined shaft angles are deformed with comparing with the straight shaft ($\psi = 0°$) and the low inclined shaft angles including the usual inclined shaft angle, $\psi < 12°$. Moreover, the amplitude of actual thrust and torque coefficients at one rotation with the high inclined shaft angles fluctuated more than those with the low inclined shaft angles. The pressure coefficient distributions on the blade at each radius with the high inclined shaft angles are mostly violent than those with the low inclined shaft angles which are corresponded to the pressure distributions on suction and pressure sides. In addition, the average velocity in downstream confirmed to have more unbalanced forces operating at high inclined shaft angles which is consistent with the pressure distribution.

The results of this study indicate that the propeller characteristics (pitch, rake and skew) and the angle of inclined shaft propeller should be considered properly to find suitable design condition for the operating inclined shaft because it is directly influent to propeller performance. In addition, it should be checked whether the propeller generates the unbalanced loading on each blade which causes the cavitation including the propeller damage and vibration.

Acknowledgement

The ANSYS Fluent software in this research work is supported by the Faculty of Engineering at Si Racha, Kasetsart University, Sri Racha Campus.

References

Alder, R.S. and Moore, D.H. (1977): Performance of an inclined shaft partially-submerged propeller operating over a range of shaft yaw angles, David W. Taylor Naval Ship Research and Development Center, Bethesda,

Maryland, USA.

Boswell, R., Jessup, S. and Kim, K-H. (1981): Periodic single blade loads on propeller is tangential and longitudinal wakes, SNAME Propellers'81 Symposium, Virginia Beach, USA. https://doi.org/10.5962/bhl.title.47327

Boswell, R., Jessup, S., Kim, K-H. and Dahmer, D. (1984): Single-blade loads on propellers in inclined and axial flows, Technical report, DTNSRDC-84/084.

Dubbioso, G, Muscari, R. and Mascio, A.D. (2013): CFD Analysis of Propeller Performance in Oblique Flow, SMP'13, Tasmania, Australia.

Jessup, S.D. (1982): Measurements of the pressure distribution on the two model propeller, David Taylor Naval Research and Development Center report, DTNSRDC-82/035. https://doi.org/10.5962/bhl.title.47357

Kaewkhiaw, P. and Ando, J. (2014): Numerical simulation for unsteady propeller performance with inclined shaft propeller arrangement using CFD, The 11th ICHD, Singapore.

Kaewkhiaw, P., Yoshitake, A., Kanemaru, T. and Ando, J. (2016): Evaluation of Thai Long-Tail Boat propeller performance and Its improvement, 12th ICHD, Netherland.

Kaewkhiaw, P. (2018): The Effect of shaft yaw angles on propeller performance for Long-Tail Boat using CFD, 13th ICHD, Incheon, South Korea.

Kinnas, S.A. and Pyo, S. (1998): The tip flows for wings and propellers and their effect on the predicted performance, Technical report of ocean engineering group, Department of Civil Engineering, The University of Texas at Austin.

Ræstad, A.E. (2007): Experimental data provided for the Norwegian Propeller Forum, Courtesy by DNV. Taniguchi, K., Tanibayashi, H. and Chiba, N. (1967): Investigation into the propeller cavitation in oblique flow, The Society of Naval Architects of Japan. https://doi.org/10.2534/jjasnaoe1952.1967.81